IMA Conference on Mathematics of Robotics
9 – 11 September 2015, St Anne's College, University of Oxford Preliminary version

A Class of 6R Robots and Poses with 16 Analytical Solutions

By Martin G. Weiß

OTH Regensburg
Faculty of Computer Science and Mathematics
Regensburg, Germany

Abstract

We describe a class of 6R robots for which we can give explicit formulas for the 16 solutions in the special case of the tool orientation in parallel with axes of the base coordinate system. This setting can serve as the starting point for research towards better understanding of the 16 solutions.

1. Introduction

It has been known for some time that a serial robot with 6 revolute joints admits at most 16 discrete solutions, e. g. Lee & Ljang (1988) and Primrose (1986). Manseur & Doty (1989) have given an example of an orthogonal 6R robot, i.e. a robot with only integer multiples of $\frac{\pi}{2}$ in the Denavit-Hartenberg-parameters, and a specific pose that admits 16 discrete solutions. This example has a TCP orientation and position probably found by extensive numerical search and does not give much insight into the structure of the solution set.

Our robot class is motivated by the KUKA Transpressor, an industrial robot designed for high-speed handling of large components in car production, like moving steel sheets from one press to another. The kinematic structure is derived from a standard 6-axis KUKA robot with kinematics similar to the well-known PUMA 560 or most 6R robots in industry, with one essential change: The axis 6 is shifted parallel from its standard location, shown in red in Figure 1, to the green location. Mechanically this is accomplished by an additional chain transmission - like a bicycle chain - in a carbon housing. Consequently the wrist is no longer a central wrist, and no analytic solution is known.

Numerical studies show that this robot can reach poses with 16 different axis configurations $\vartheta^{(1)}, \ldots, \vartheta^{(16)} \in \mathbb{R}^6$ although in reality far less can be realized due to mechanical constraints $\vartheta_{i,\min} \leq \vartheta_i \leq \vartheta_{i,\max}$.

We present a simplified robot motivated by the Transpressor, and poses with 16 intuitive solutions for the backward transform which can be written down explicitly. We also motivate why research should investigate the problem of the definition of a set of "status" bits for the general 6R robot structure because otherwise these types will be plagued by severe drawbacks.

2. Kinematic Structure and a 16 Solution Pose

We consider a 6R robot with the kinematic structure defined in standard Denavit-Hartenberg parameters as in Corke (2011) where the values given in Table 1 are not

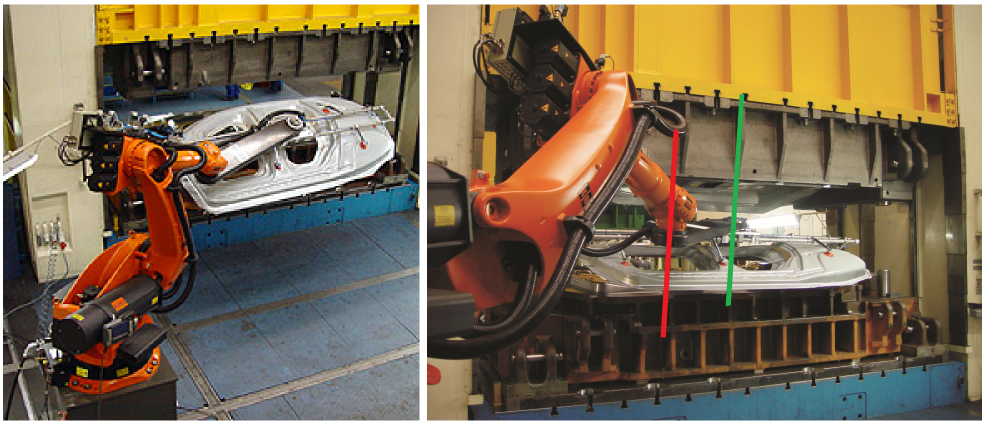

FIGURE 1. KUKA Transpressor robot

i	d_i	a_i	α_i
1	200	0	$\frac{\pi}{2}$
2	0	600	0
3	0	0	$-\frac{\pi}{2}$
4	500	0	$\frac{\pi}{2}$
5	0	130	$-\frac{\pi}{2}$
6	0	0	0

TABLE 1. Denavit-Hartenberg parameters

the original ones. The value $a_5 \neq 0$ is crucial as it results in a non-central wrist, giving the offset of the wrist extension. All angles α_i are multiples of $\frac{\pi}{2}$ to give a orthogonal robot in the terminology of Manseur & Doty (1989). The principle behind the constructed pose does not depend on special numerical values otherwise, basically we need non-zero lengths a_2, d_4, a_5 only. With the abbreviation $A_i(\vartheta_i) = \mathrm{R}_z(\vartheta_i)\mathrm{T}_z(d_i)\mathrm{T}_x(a_i)\mathrm{R}_x(\alpha_i)$ we have the tool centre point

$$\mathsf{TCP}(\vartheta) = A_1(\vartheta_1)A_2(\vartheta_2)A_3(\vartheta_3)A_4(\vartheta_4)A_5(\vartheta_5)A_6(\vartheta_6)$$

expressed relative to the world coordinate system W which is chosen as the axis 1 coordinate system. The axes of rotation of the joints will be denoted $z_1, \ldots, z_6$, with the other axes in the Denavit-Hartenberg coordinates system x_i and y_i.

The zero pose $\vartheta = 0 \in \mathbb{R}^6$ of the robot is shown in Figure 2†. The red dot on the left side symbolizes a machanical marker that rotates with axis 1. It will be used to denote axis 1 angles as "left", "right", "front" and "back". Mechanically this "mastering marker" defines $\vartheta_1 = 0$ relative to the ground. The configuration of Figure 2 will be termed left for obvious reasons. The right, front and back configurations then correspond to $\vartheta_1 = \pi$, $\vartheta_1 = -\frac{\pi}{2}$ and $\vartheta_1 = \frac{\pi}{2}$ respectively. We consider the TCP as a function defined for $\vartheta \in (-\pi, \pi]^6 =: \Theta$ although in reality mechanical restrictions $\vartheta_i \in [\vartheta_{i,\min}, \vartheta_{i,\max}]$ apply.

† All figures were created using the MATLAB Robotics Toolbox described in Corke (2011).

IMA Conference on Mathematics of Robotics
9 – 11 September 2015, St Anne's College, University of Oxford Preliminary version

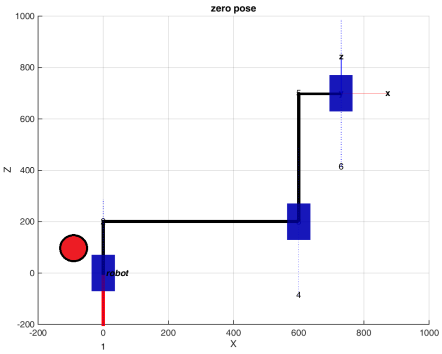

FIGURE 2. Orthogonal Robot with non-central wrist

The pose with 16 solutions now is defined relative to the world by

$$^{\mathsf{W}}\mathsf{TCP} = \begin{bmatrix} 0 & 0 & 1 & 0 \\ 0 & 1 & 0 & 0 \\ -1 & 0 & 0 & \tilde{z} \\ 0 & 0 & 0 & 1 \end{bmatrix} \tag{2.1}$$

The height $\tilde{z}$ is a parameter in the construction, giving a family of 16 solution poses. For the figures we define $z = \tilde{z} - d_1$: If we choose $d_1 = 0$ then $z = \tilde{z}$ and the TCP is located in the origin of the world and axis 1 coordinate system. We have chosen $d_1 \neq 0$ because otherwise the graphical presentation would be an overlay of too many axes at essential points.

The ideas behind this pose are the following: If the TCP is located on z_1 and $\vartheta_1 = 0$, then the x_5 axis, i.e. the wrist extension, can be aligned with z_1 by a suitable value of ϑ_5. The x-axis of the TCP then coincides with the negative z_1 direction as required by (2.1), and axis 6 can align the y- and z-axes of the TCP. The alignment of z_1 and the wrist extension can occur upwards or downwards, depending on $\vartheta_4 = 0$ or $\vartheta_4 = \pi$: this gives 2 solutions, see the two configurations in Figure 3. The angles α, β, γ are calculated by the law of cosines. Similar to a Puma-like robot, joints 2 and 3 can create 2 symmetric solutions, the second one shown in gray in the figures. The point positioned here is not the wrist centre point but only the intersection of z_4 and z_5. Another 2 solutions are given when $\vartheta_1 = \pi$: Due to the symmetry of our robots the pictures would look exactly the same but for the orientation of the intermediate coordinate systems.

So far we have obtained 8 solutions. Another 8 different solutions are located in what we call "front" and "back" position $\vartheta_1 = \pm\frac{\pi}{2}$, see Figure 4. Here also $\vartheta_4 = \pm\frac{\pi}{2}$, $\vartheta_5 = \pm\frac{\pi}{2}$ such that z_4 and x_5 are aligned. Now, when ϑ_2 and ϑ_3 position the centre of the last coordinate system on z_1, then z_6 is pointing in the x_1-direction, and a suitable rotation ϑ_6 aligns x_6 and y_6 as desired. As in the left and right case, a flip of axis 5 creates two solutions, where the connection from joint 3 to joint 4 with length d_4 is extended or shortended by a_5, see Figure 4. Again, two triangles in the joints 2 and 3 are possible.

Note that α, β, γ depend on the configuration. A necessary and sufficient condition for the existence of 16 solutions is that the construction of the triangles $\Delta(a, b, c)$ is possible (where a is the side opposite of α and so on), i.e. the sum of any two sides is strictly larger than the third side:

$\Delta(d_4, z + a_5, a_2) \mapsto (\alpha^{(1)}, \beta^{(1)}, \gamma^{(1)})$ left and right, extension down, no wrist flip

$\Delta(d_4 + a_5, z, a_2) \mapsto (\alpha^{(2)}, \beta^{(2)}, \gamma^{(2)})$ back and front, no wrist flip

IMA Conference on Mathematics of Robotics
9 – 11 September 2015, St Anne's College, University of Oxford Preliminary version

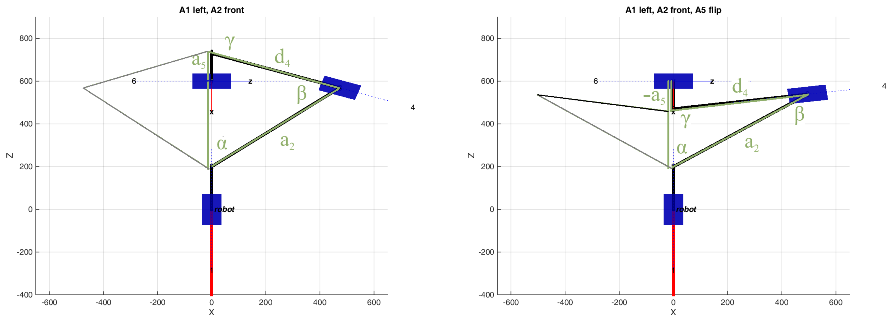

FIGURE 3. Left and right configurations of the robot

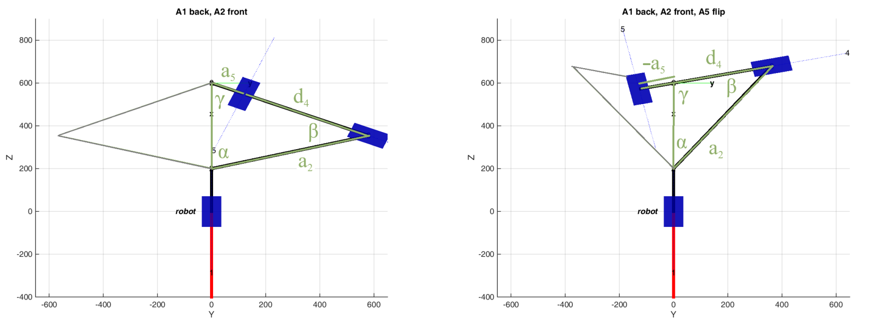

FIGURE 4. Front and back configurations of the robot

$\Delta(d_4, z - a_5, a_2) \mapsto (\alpha^{(3)}, \beta^{(3)}, \gamma^{(3)})$	left and right, extension up, wrist flip
$\Delta(d_4 - a_5, z, a_2) \mapsto (\alpha^{(4)}, \beta^{(4)}, \gamma^{(4)})$	back and front, wrist flip

With these definitions one can define the 16 poses of Table 2 by elementary sign considerations. The poses are locally unique as numerical computation of the rank of the Jacobian J or of the determinant of $J^t J$ shows. Figures 5 to 8 show the poses for $\tilde{z} = 600$.

3. Generalization, Practical Relevance and an Open Problem

Also the robot's Denavit-Hartenberg parameters of Table 1 can be generalized to $a_1 \neq 0$ and $a_3 \neq 0$. Then the symmetry in the front and back configuration of axis 2 and 3 is lost: one has to construct quadrangles instead of triangles, but still 16 poses exist for suitable lengths.

By variation of z some or all of the symmetric triangles degenerate to a single line or are not constructible any more. So we can define TCP-positions with any number between 0 and 16 solutions on axis 1 (this requires $a_1 \neq 0$ as otherwise always 2 symmetric left and right solutions would disappear simultaneously).

The 16 solutions not only exist on the z_1-axis but also for TCP frames in a neighbourhood of (2.1). Numerical computation shows that the solutions can still be classified in the regions seen so far: ϑ_1 in one of 4 sectors, ϑ_2 (or ϑ_3) front or back, wrist flipped or not. Continuation schemes will calculate all solutions but cannot deliver this classification as – in contrast to a Puma-like kinematic – we do not know an analytical solution or the boundaries defined by singularieties between the partition of $(-\pi, \pi]^6$ into the 16

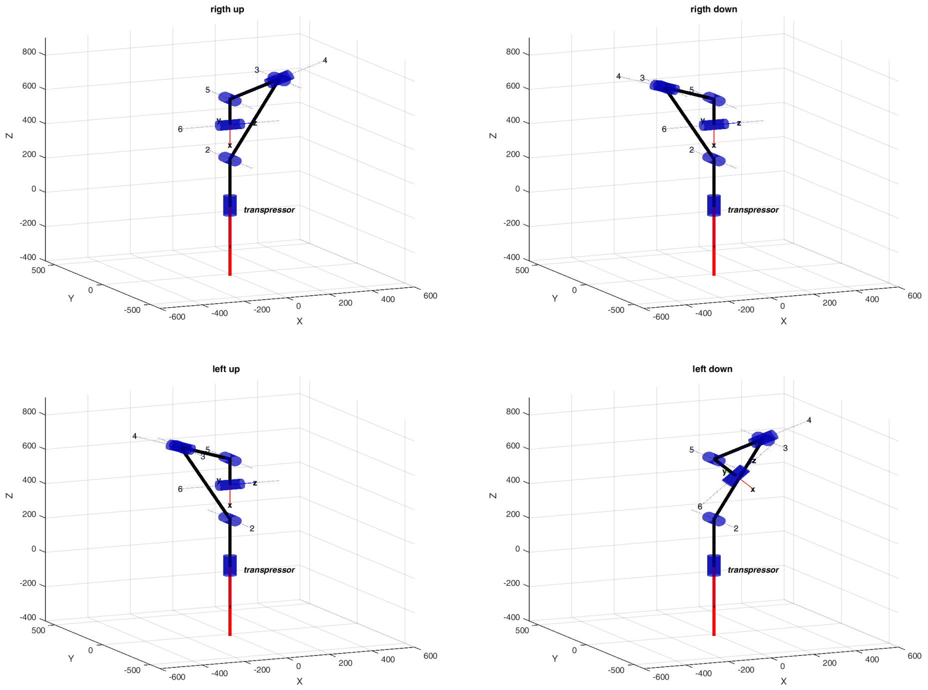

FIGURE 5. 4 Poses in left / right configuration

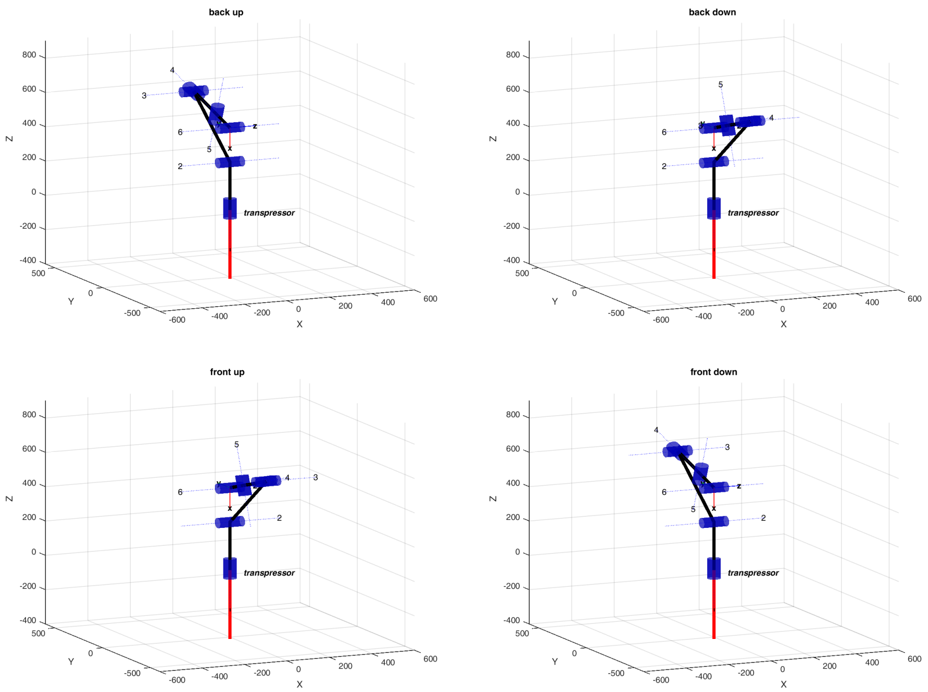

FIGURE 6. 4 Poses in front / back configuration

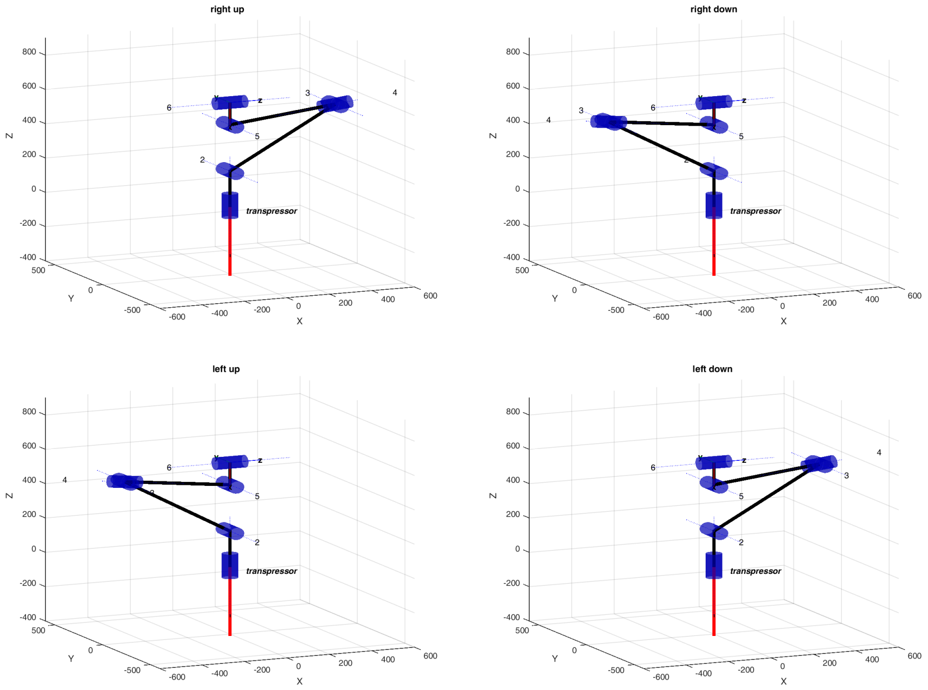

FIGURE 7. 4 Poses in left / right configuration, wrist up

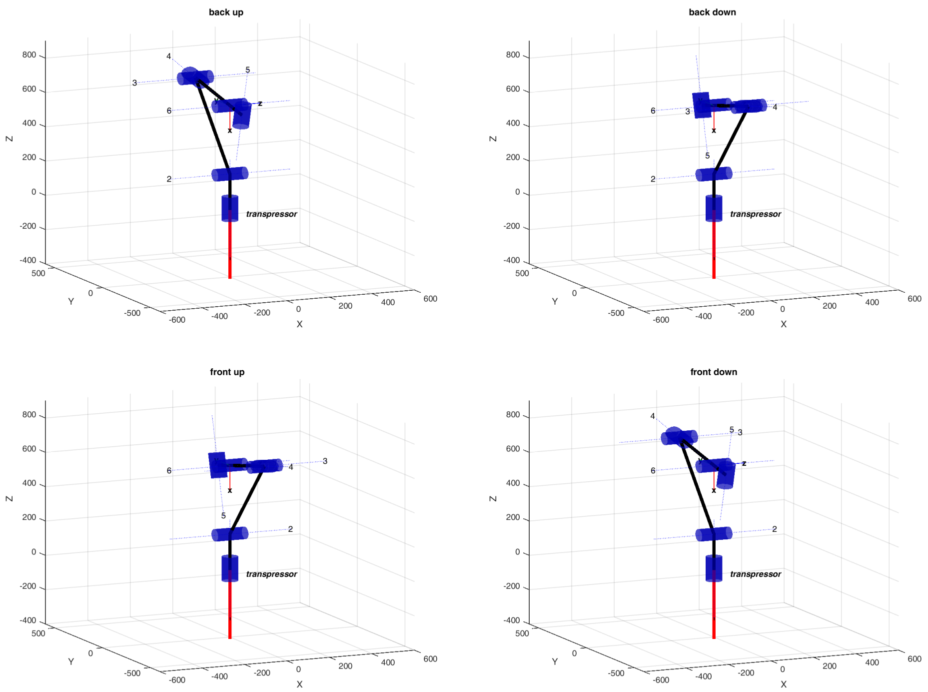

FIGURE 8. 4 Poses in front / back configuration, wrist up

pose	ϑ_1	ϑ_2	ϑ_3	ϑ_4	ϑ_5	ϑ_6	description
1	0	$\frac{\pi}{2}-\alpha^{(1)}$	$\frac{\pi}{2}-\beta^{(1)}$	0	$-\frac{\pi}{2}-\gamma^{(1)}$	0	A1 left, A2 front
2	0	$\frac{\pi}{2}+\alpha^{(1)}$	$\frac{\pi}{2}+\beta^{(1)}$	0	$-\frac{\pi}{2}+\gamma^{(1)}$	0	A1 left, A2 back
3	π	$\frac{\pi}{2}-\alpha^{(1)}$	$\frac{\pi}{2}-\beta^{(1)}$	π	$-\frac{\pi}{2}+\gamma^{(1)}$	0	A1 right, A2 front
4	π	$\frac{\pi}{2}+\alpha^{(1)}$	$\frac{\pi}{2}+\beta^{(1)}$	π	$-\frac{\pi}{2}-\gamma^{(1)}$	0	A1 right, A2 back
5	$\frac{\pi}{2}$	$\frac{\pi}{2}-\alpha^{(2)}$	$\frac{\pi}{2}-\beta^{(2)}$	$\frac{\pi}{2}$	$\frac{\pi}{2}$	$\pi-\gamma^{(2)}$	A1 back, A2 front
6	$\frac{\pi}{2}$	$\frac{\pi}{2}+\alpha^{(2)}$	$\frac{\pi}{2}+\beta^{(2)}$	$\frac{\pi}{2}$	$\frac{\pi}{2}$	$\pi+\gamma^{(2)}$	A1 back, A2 back
7	$-\frac{\pi}{2}$	$\frac{\pi}{2}-\alpha^{(2)}$	$\frac{\pi}{2}-\beta^{(2)}$	$-\frac{\pi}{2}$	$\frac{\pi}{2}$	$\pi+\gamma^{(2)}$	A1 front, A2 front
8	$-\frac{\pi}{2}$	$\frac{\pi}{2}+\alpha^{(2)}$	$\frac{\pi}{2}+\beta^{(2)}$	$-\frac{\pi}{2}$	$\frac{\pi}{2}$	$\pi-\gamma^{(2)}$	A1 front, A2 back
9	0	$\frac{\pi}{2}-\alpha^{(3)}$	$\frac{\pi}{2}-\beta^{(3)}$	π	$\frac{\pi}{2}+\gamma^{(3)}$	π	A1 left, A2 front, A5 flip
10	0	$\frac{\pi}{2}+\alpha^{(3)}$	$\frac{\pi}{2}+\beta^{(3)}$	π	$\frac{\pi}{2}-\gamma^{(3)}$	π	A1 left, A2 back, A5 flip
11	π	$\frac{\pi}{2}-\alpha^{(3)}$	$\frac{\pi}{2}-\beta^{(3)}$	0	$\frac{\pi}{2}-\gamma^{(3)}$	π	A1 right, A2 front, A5 flip
12	π	$\frac{\pi}{2}+\alpha^{(3)}$	$\frac{\pi}{2}+\beta^{(3)}$	0	$\frac{\pi}{2}+\gamma^{(3)}$	π	A1 right, A2 back, A5 flip
13	$\frac{\pi}{2}$	$\frac{\pi}{2}-\alpha^{(4)}$	$\frac{\pi}{2}-\beta^{(4)}$	$-\frac{\pi}{2}$	$-\frac{\pi}{2}$	$-\gamma^{(4)}$	A1 back, A2 front, A5 flip
14	$\frac{\pi}{2}$	$\frac{\pi}{2}+\alpha^{(4)}$	$\frac{\pi}{2}+\beta^{(4)}$	$-\frac{\pi}{2}$	$-\frac{\pi}{2}$	$+\gamma^{(4)}$	A1 back, A2 back, A5 flip
15	$-\frac{\pi}{2}$	$\frac{\pi}{2}-\alpha^{(4)}$	$\frac{\pi}{2}-\beta^{(4)}$	$\frac{\pi}{2}$	$-\frac{\pi}{2}$	$+\gamma^{(4)}$	A1 front, A2 front, A5 flip
16	$-\frac{\pi}{2}$	$\frac{\pi}{2}+\alpha^{(4)}$	$\frac{\pi}{2}+\beta^{(4)}$	$\frac{\pi}{2}$	$-\frac{\pi}{2}$	$-\gamma^{(4)}$	A1 front, A2 back, A5 flip

Table 2. 16 Poses for one TCP position

solution sets. However this 4 bit classification of the solutions is essential for industrial robot controller where positions are given by frames and some discrete "status" bits, that is a finite set $S = \{s_1, \ldots, s_M\}$, here $M = 16$, such that the backward transform of a frame-status pair (F, s), F a frame and $s \in S$, is unique for all but the singular configurations, combined with an algorithmic or geometric interpretation of the partition. Without such a status definition, one has no way to predict what the axis configuration will be, how to avoid singularities, or how to keep the status constant during cartesian motions.

This remains an open question, and I would not be surprised if no explicit status definition and no explicit solution formula could be given although I know of no proof that a general orthogonal 6R robot is not solvable in the sense of Galois theory. The degree 16 in classical polynomial based approaches like Li & Wörnle & Hiller (1989) or Gröbner base methods like Wang & Hang & Yang (2006) is a strong hint in direction of non-solvability but the polynomials are far too complicated to be understood for a general TCP frame. So it might be worth looking at this robot class with the eyes the newer solution approaches of Husty & Pfurner & Schroecker (2007) or Selig (2007).

4. Conclusion

We have presented a class of robots closely resembling an industrial robot that gives rise to 16 solutions for a wide range of parameters. For a pose parallel to the world coordinate system the solution process consists of triangle constructions, or quadrangle constructions if a slightly more general robot class with offset in the main axes is considered.

Although elementary in construction, to the best of the author's knowledge no 6R robot has been reported where all 16 solutions of the backward transform can be given analytically. The solution set suggests that the solutions can be classified by a status composed of 4 bits representing sign decisions, but this could not shown in general.

REFERENCES

Corke, Peter I. 2011 Robotics, Vision & Control: Fundamental Algorithms in Matlab, Springer

KUKA Systems `http://www.kuka-systems.com/en/products/industrial_solutions/press_automation/products`

Husty, M.L. & Pfurner, M. & Schroecker, H.-P. 2007, A new and efficient Algorithm for the Inverse Kinematics of a General Serial 6R Manipulator, *Mech. Mach. Theory* **42(1)**, 66–81.

Lee, H.Y. & Liang, C.G. 1988, Displacement analysis of the general spatial seven-link 7R mechanism, *Mechanism and Machine Theory* **23(3)**, pp. 219226.

Li, H., Wörnle, C. & Hiller, M. 1989 A complete solution for the inverse kinematic problem of the general 6R robot manipulator, *ASME J. Mechanical Design* **113**, 481–486.

Manseur, R. & Doty, L. K. 1989 A Robot Manipulator With 16 Real Inverse Solution Sets. *International Journal of Robotics Research* **8(5)**, 75-79.

Primrose, E.J.F. 1986, On the input-output equation of the general 7R mechanism, *Mechanism and Machine Theory 21*, **6**, pp. 509510.

Selig, J.M. 2007 Geometric Fundamentals of Robotics. Springer

Wang, Y., Hang, L. & Yang, T. 2006 Inverse Kinematics Analysis of General 6R Serial Robot Mechanism Based on Groebner Base, *Front. Mech. Eng. China* **1**, 115–124.